A Whole-Body Compliance Control Strategy of Truss Crawling for Multi-Arm Space Robots

Zijian Dai[1], Peiji Wang[1](✉), Tao Lin[2], and Chengfei Yue[1]

[1] Harbin Institute of Technology Shenzhen, Shenzhen 518055, China,
wangpeiji@hit.edu.cn,
[2] Harbin Institute of Technology, Harbin 150001, China

Abstract. The on-orbit service technologies such as on-orbit assembly, inspection and maintenance of large spacecraft have become significant development direction in the future. Multi-arm space robots, capable of high-risk and high-load tasks, can move on the space truss and complete on-orbit assembly and maintenance tasks. These robots have broad application prospects in on-orbit services, where their precise and stable movement capabilities are crucial for mission success. However, during contact motion and closed-loop motion, the lack of compliance in multi-arm space robots may result in excessive force or torque on the target, potentially damaging the robot itself or the spacecraft equipment. Therefore, we propose a whole-body compliance control strategy (WBCC) for the motion of multi-arm space robots to reduce the risks of space truss crawling. The WBCC includes a unified compliance model consisting of a cartesian compliance model for the ends and a virtual spring model of the floating base. We use the MPC method to optimize the contact force of the effector to solve contact stability problem caused by the interaction between the robot and the rigid truss. Also, we embed it in the WBCC to ensure the motion stability during crawling. Finally, we verify the control strategy in Isaac Sim, and the simulation results indicate that the strategy can achieve compliance control for multi-arm robots during space truss crawling.

Keywords: on-orbit service, multi-arm space robots, space truss crawling, compliance control

1 Introduction

In the process of on-orbit services such as on-orbit assembly and space station maintenance, astronauts who go out of the capsule for a long time will consume a lot of physical energy and face great personal safety risks. While, the multi-arm space robots have significant advantages in terms of stability, flexibility, and carrying capacity [1]. The ability to perform tasks safely for a long time is an effective solution to reduce astronauts' workload and their potential operational risks.

In typical long-term on-orbit service, such as repairing or refueling spacecraft, space debris handling and on-orbit assembly, multi-arm space robots often

move to the working location by crawling space trusses [2]. Due to the unique zero-gravity environment in space, any internal stress or collision during the crawling process could potentially damage both the robot and the spacecraft. Therefore, the dynamic motion of multi-arm robots in space is a very complex issue, involving multi-body systems interacting with the environment through multiple support points and requiring precise motion and force control schemes [3]. In order to solve such problems, multi-arm space robots are required to have the capability to compliantly interact with the environment during motion, similar to quadruped robots on Earth, we refer to this capability as compliance. In the early development of active compliance control methods, the focus was on designing algorithms to control the rigid movements of robot legs to achieve compliant contact with the environment. Consequently, impedance control was extensively used in the active compliance control of legged robots [4]. Based on the working space, leg impedance control is mainly divided into joint space [5], polar coordinate space [6], and Cartesian space [7]. Subsequently, Pratt et al. proposed the concept of Virtual Model Control (VMC) to address the compliance and stability needs of floating bodies, applying active compliance control to the compliant interaction and stability control of six-DOFs floating bodies [8]. By applying a virtual spring-damper model in the floating body and inertial coordinate system, they achieved compliance control for the posture adjustment of the body and dynamic compliant interaction between the legged robot and the ground [9]. VMC can be appropriately adjusted according to the requirements to realize many different control effects. Chen et al. established VMC model of the legged robot with trot gait and achieved the dynamic internal force balance of a multi-body system [10]. Additionally, Xie et al. optimized the desired contact force at the foot end of a quadruped robot equipped with a six-DOFs robotic arm using VMC by compensating the arm's inertia, finally achieved the quadruped robot's compliant adaptation to the external disturbances [11].

However, the above active compliance control methods are not entirely suitable for multi-arm robots crawling in space, because the end contact tolerance for multi-arm robots in space differs significantly from that of quadruped robots on the ground. Quadruped robots have a larger contact tolerance, and the open ground space provides them with more options for foothold selection. Due to the presence of gravity, we can control the centers of gravity of quadrupedal robots by methods such as the ZMP inverted pendulum [12], which have the ability to keep the robot's whole-body internal forces in a well converged and balanced state. However, the multi-arm space robots need to alternately gripping with end effectors to achieve truss crawling, and the change of contact force and attitude incoordination of the robot without gravity constraints will greatly affect the balance of internal forces in the whole body of the robot [13]. Additionally, a slight contact error in the effector space during crawling can lead to contact instability problems, which generates large contact force variations that will lead to the damage of robot or spacecraft [14]. Therefore, the zero-gravity environment in space and the characteristics of multi-arm robot crawling impose higher requirements on end contact constraints compared to quadruped robots.

To solve these problems, we propose a whole-body compliance control strategy (WBCC) for multi-arm robots to achieve compliance control during space truss crawling.

Our main contributions are:

1. We establish a unified whole-body compliance model through the force mapping relationship from the end effector to the floating base, solving the problem of crawling posture coordination for robots in the zero-gravity environment.

2. Based on achieving whole-body compliance for the multi-arm robots, we introduce the MPC control law and utilize its excellent real-time performance, state constraint capabilities to meet the higher requirements of space crawling and ensure the contact stability of the multi-arm robots' end effectors with the space truss.

2 Whole-Body Compliance Control Strategy

While crawling in space, multi-arm robots need to maintain stable motion and compliance interaction. Therefore, we proposes a Cartesian compliance model of the clamping end and a compliance model of the floating base from the perspectives of the end and the floating base, and establishes a unified whole-body compliance model by analyzing the force mapping relationship between them. The MPC external frame is used to ensure the contact stability through keeping the clamping force of effectors within a safe range during crawling.

2.1 Modeling of Multi-Arm Space Robots

We established the corresponding coordinate system for each joint by DH methods for the four-arm space robot which is designed by ourselves. The global axis is O_g , the axis for each joint is O^i_{Jk} and the axis at each end is O^i_E , where $i \in \{1, 2, 3, 4\}, k \in \{1, \cdots, 7\}$. Our four-arm space robot and the scene of crawling on the space truss is depicted in Fig. 1.

This inertial axis ensures unity of whole-body motion framework. Based on these, the velocity-level kinematics of the branch arm are as follows:

$$\dot{q} = J^{-1} \cdot \begin{bmatrix} v_e \\ \omega_e \end{bmatrix} \tag{1}$$

where $\dot{q}$ is generalized velocity of joints, v_e and ω_e are velocity and angular velocity of effectors of branch arms.

The generalized displacement q consists of displacement of the base, Euler angles, and joint displacements of four branch arms.The generalized velocity v consists of linear and angular velocities of base and joint velocities of each of four branch arms. The dynamic equation of the multi-arm space robot is as follows:

$$D(q)\ddot{q} + H(q, \dot{q})\dot{q} = J_S^T \lambda + \tau \tag{2}$$

where $D(q)\ddot{q}$ describes inertial torque of robots, $H(q, \dot{q})\dot{q}$ describes centrifugal and Coriolis effect, τ describes joint driven torque during the motion gait, and $J_S^T \lambda$ describes external force on robots.

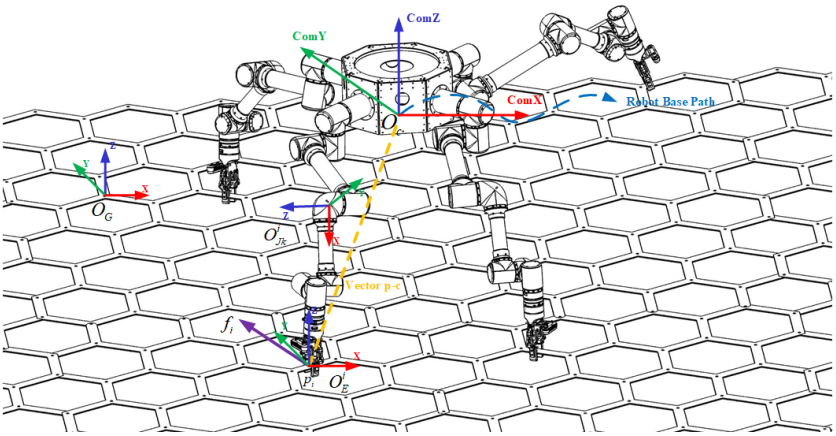

Fig. 1. Scene of a four-arm space robot crawling on the space truss

2.2 Whole-Body Compliance Model

The design of the whole body compliance model is divided into two parts: the end-cartesian compliance model and the floating base compliance model, which are connected by force maps.

End-Cartesian Compliance Model. The dynamic interaction during crawling is mainly reflected in the unstable mutual contact process between the effectors and the space truss. Therefore, it is necessary to establish the linear mapping of the interaction force of the effectors to improve the compliant motion characteristics of multi-arm robots. The end-cartesian impedance model of multi-arm space robots is depicted in Fig. 2.

effector motion interaction process of a branch arm in Cartesian space is depicted in Fig. 2. The trajectory of the effectors of the four-arm robot is simplified and reduced to a straight line trajectory, which focuses on the effect of the robot after interacting with the space trusses. As a result, according to the impedance model in Cartesian space, the basic compliance model of the interaction force at its holding arm can be expressed as:

$$f_i^d - f_i = K_i\left(p_i^d - p_i\right) + B_i\left(\dot{p}_i^d - \dot{p}_i\right) + M_i\left(\ddot{p}_i^d - \ddot{p}_i\right) \tag{3}$$

where f_i^d is the expected end force in the y direction; f_i is force feedback of effector in the y direction; K_i is the rigidity parameter, which mainly affects the elasticity of the arm; B_i is the damping parameter, which mainly affects the damping characteristics of the arm, and M_i is the inertia parameter, which mainly affects the inertia characteristics of the arm.

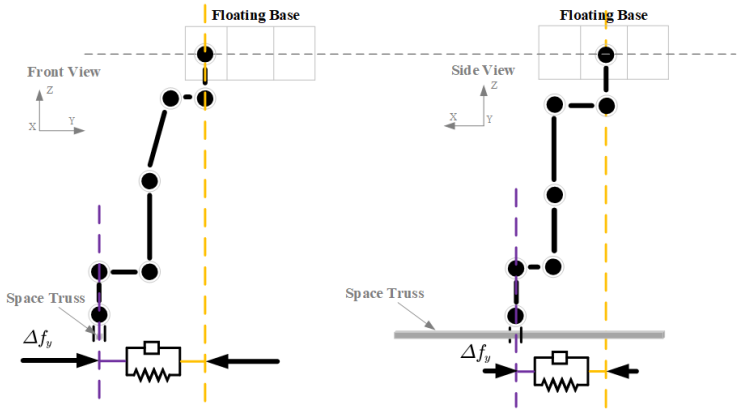

Fig. 2. Impedance model of the effectors in cartesian space

Thus, we get a simplified form of the end-cartesian model of compliance as follows:

$$f_i^d = f_i + C \cdot \Delta p_i \tag{4}$$

where $\Delta \dot{p}_i = \dot{p}_i^d - \dot{p}_i$ and C is the admittance matrix obtained by Eq. (3).

Floating Base Compliance Model. For space robots, the six-dimensional virtual force/torque of the whole body compliance model cannot be directly controlled, it depends on the force map between the clamping effector and the base. Therefore, the key to the whole-body compliance control is to establish the mechanical mapping relationship between the end-cartesian compliance model and the virtual spring of the floating base, the force mapping of them is as follows:

$$\begin{cases} f_c = \sum_{i=1}^{4} f_i \\ \tau_\theta = \sum_{i=1}^{4} (p_i - c) \times f_i \end{cases} \tag{5}$$

where p_i is the position of the robot clamping point on the truss in Fig. 1, and c is the location of center of mass.

We find that normal force of effectors of multi-arm space robots has a great influence on the crawling stability, so the main establishment of the force mapping relationship of the floating base is simplified to the influence effect of the normal force, that is, the yaw, roll and y position. Compliance model of the floating base is depicted in Fig. 3:

Based on the above, force generated at the clamping effector is equated to the moments of center around x-axis, around z-axis, and force along y vertical direction. Therefore, the force mapping relationship in the above can be further

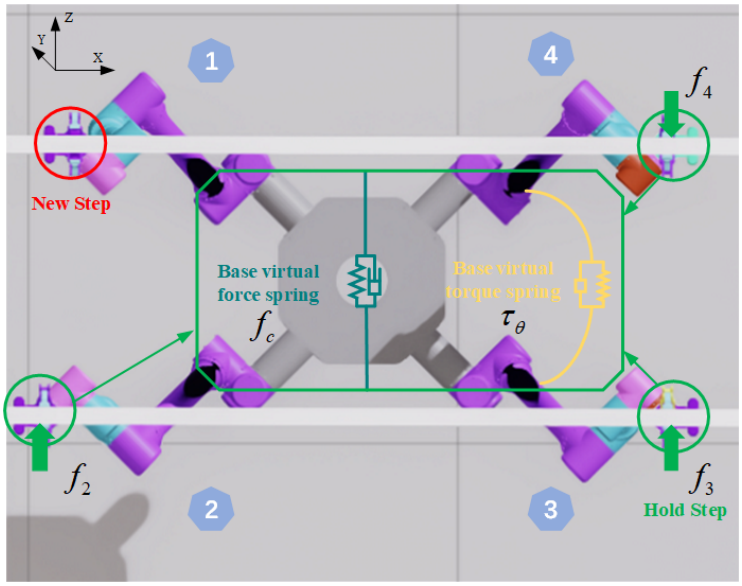

Fig. 3. Virtual spring model of floating base

expanded:

$$\begin{aligned} K_F^Y\left(y_d-y\right)+B_F^Y\left(\dot{y}_d-\dot{y}\right)+M_F^Y\left(\ddot{y}_d-\ddot{y}\right)&=\sum_{i=1}^4 f_i^d\cdot s_i \\ K_T^Y\left(\alpha_d-\alpha\right)+B_T^Y\left(\dot{\alpha}_d-\dot{\alpha}\right)+M_T^Y\left(\ddot{\alpha}_d-\ddot{\alpha}\right)&=\sum_{i=1}^4\left(p_{ix}-c_x\right)\cdot f_i^d\cdot s_i \\ K_T^R\left(\beta_d-\beta\right)+B_T^R\left(\dot{\beta}_d-\dot{\beta}\right)+M_T^R\left(\ddot{\beta}_d-\ddot{\beta}\right)&=\sum_{i=1}^4\left(p_{iz}-c_z\right)\cdot f_i^d\cdot s_i \end{aligned} \tag{6}$$

where y_d is expected y-direction position of base, y is actual y-direction position of base, α_d is expected base roll angle, α is the actual base roll angle, β_d is the expected base yaw angle, β is the actual base yaw angle, K_F^Y, K_T^Y, K_T^R are the stiffness parameters of the y-direction, roll and yaw of the base compliance model, and B_F^Y, B_T^Y, B_T^R are the damping parameters of these three dofs, B_F^Y, B_T^Y, B_T^R are the inertia parameters and $s_i \in \{0,1\}$, which represents the flags of the moving phase (0) and the clamping phase (1) of the branch arm.

Therefore, we get a simplified form of the compliance model of the floating base as follows:

$$D\cdot\Delta\dot{b}=G\cdot f_i^d\cdot s_i \tag{7}$$

where $\Delta\dot{b}=\left\{\dot{y}_d-\dot{y},\dot{\alpha}_d-\dot{\alpha},\dot{\beta}_d-\dot{\beta}\right\}$, D and G are the base spring matrix and force distribution matrix obtained from Eq. (6).

Above all, we discuss the influence of the terminal normal force of the space robot when crawling on the truss, simplify it to the y-direction, roll, and yaw three degrees of freedom force/torque, and establish the end-cartesian compliance model Eq. (4) and the floating base compliance model Eq. (7). From the above model, we design the input desired posture/position of base and output joint velocity, so the mapping of whole-body compliance model can be finally summarized as follows:

$$\Delta\dot{p}_i = \frac{D \cdot \Delta\dot{b} - G \cdot f_i \cdot s_i}{G \cdot C \cdot s_i} \tag{8}$$

2.3 MOTION OPTIMIZATION

MPC-based Force Optimization. The end of the robot during the crawling process gripping phase needs to maintain stable contact. To this end, we addresses the need for an end-flexing model for four-arm robot space truss crawling by utilizing the excellent state constraints and state output performance of the MPC control law.

According to the above Fig. 3 basic impedance control model, $\dot{p} = \dot{p}_0 + \Delta\dot{p}$ modifies the Cartesian velocity reference, we get the velocity $\Delta\dot{p}$ from the compliance model as the control input for the robot system. Therefore, we set the state vector as:

$$x = \begin{bmatrix} x_1 \\ x_2 \\ x_3 \end{bmatrix} = \begin{bmatrix} q_i \\ \dot{q}_i \\ f_i \end{bmatrix} \tag{9}$$

According to the Cartesian velocity offset $\Delta\dot{p}$ of the command, we use the counter-velocity kinematics of the manipulator. Assuming a non-singular configuration, it is described by the following :

$$\dot{q}_i = J^{-1}(q)\dot{p}_i \tag{10}$$

Bringing this into Eq. (9). we get:

$$\begin{aligned} \dot{x}_2 &= -x_2 + J^{-1}\dot{p}_0 + J^{-1}\Delta\dot{p}_i. \\ \dot{x}_3 &= -x_3 + f_i. \end{aligned} \tag{11}$$

We bring in the end forces, the robot's dynamics at the clamping end can be summarized as:

$$\begin{aligned} x^{k+1} &= Ax^k + B^k \Delta\dot{p}_i^k + M^k \dot{p}_0 + \gamma^k, \\ A &= \begin{bmatrix} I_N & I_{N_{\text{dor}}} & \mathbf{0} \\ \mathbf{0} & I_{N_{\text{dor}}} & \mathbf{0} \\ \mathbf{0} & \mathbf{0} & I_{N_{\text{effector}}} \end{bmatrix} \\ B^k &= \begin{bmatrix} \mathbf{0} \\ J^{-1}\left(x_1^k\right) \\ \mathbf{0} \end{bmatrix}, \\ M^k &= B^k, \\ \gamma^k &= \begin{bmatrix} 0 \\ 0 \\ f_i \end{bmatrix} \end{aligned} \tag{12}$$

We summarize this as the MPC problem:

$$\begin{aligned} \min_{\Delta\dot{p}} \; & \textstyle\sum_{i=1}^{N} \left(x^i - x_0\right)^\top Q \left(x^i - x_0\right) + \Delta\dot{p}^{i\top} R \Delta\dot{p}^i \\ & + \left(x^N - x_0\right)^\top Q \left(x^N - x_0\right), \\ \text{s.t.} \quad & x_{k+1} = Ax_k + B^k \Delta\dot{p}^k + M^k \dot{p}_0 + \gamma^k, \quad \forall k \in \{1, \ldots, N-1\}, \\ & \left|f_{\text{lim},j}\right| \leq \left|f_{\max,i}\right|, \forall j = 1, \ldots, N_{\text{effector}}, \\ & \left|f_{\text{climb},i}\right| < \left|f_{\text{lim},j}\right|, \forall j = 1, \ldots, N_{\text{effector}}, \end{aligned} \tag{13}$$

Constraints reflect two basic requirements for stable robot crawling: the need to maintain its effectors' velocity suitable for crawling motion, and to limit the contact force within a safe range. From this we obtain the whole-body compliance control framework for multi-arm space robots crawling on a space truss as shown in Fig. 4:

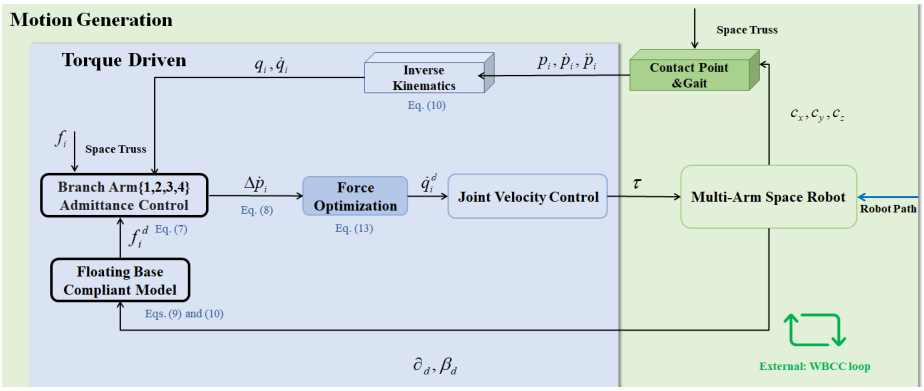

Fig. 4. Whole-body compliance control loop

3 Simulation

3.1 Setup

The model for our experimental simulation is based on a self-developed space robot, a four-armed robotic ground simulation robot with attached end force feedback. The overall simulation environment uses Isaac Sim 2023.1.0 for kinematics and environmental collision simulation, ROS2 as the communication framework, and a control frequency of 500 HZ.

3.2 Whole-Body Compliance Model

The experiments were performed using a walk gait with a velocity of approximately 10 cm/s and a phase difference of pi/4 between each leg , with four legs swinging sequentially at 4231 shown in Fig. 5. The initial force is balanced, and clamping force of the four effectors is maintained at about 20 N on average shown in Fig. 7.

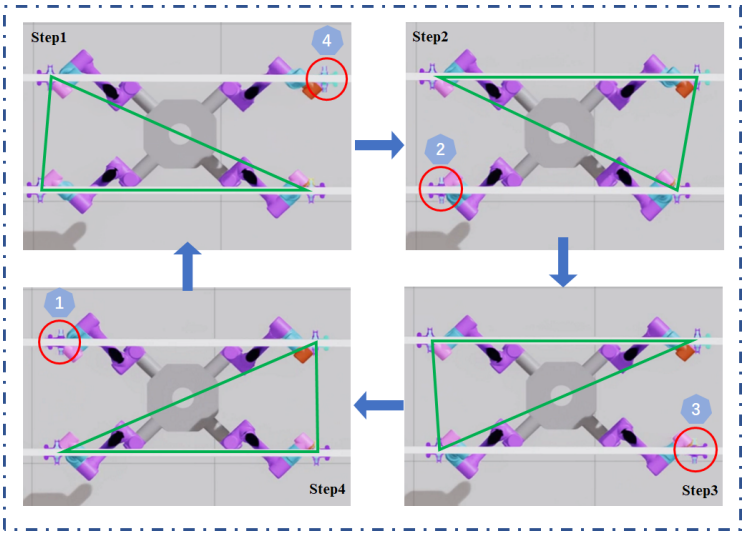

Fig. 5. Robot space truss crawl scene: walk gait {4231}

With the start of the gait, the average force of the four effectors increases due to the crawling motion and the deviation of the clamping point. As a direct result of this increase in undesirable forces at the ends, the yaw and roll angles of the base in Fig. 8 are in a gradual divergence (up to 0.05 rad and -0.03 rad respectively in the first cycle), which is also in line with Eq. (2), and this divergence will lead to the instability of the robot crawling and eventually even break away from the truss. In the two gait phase, the support leg changes from

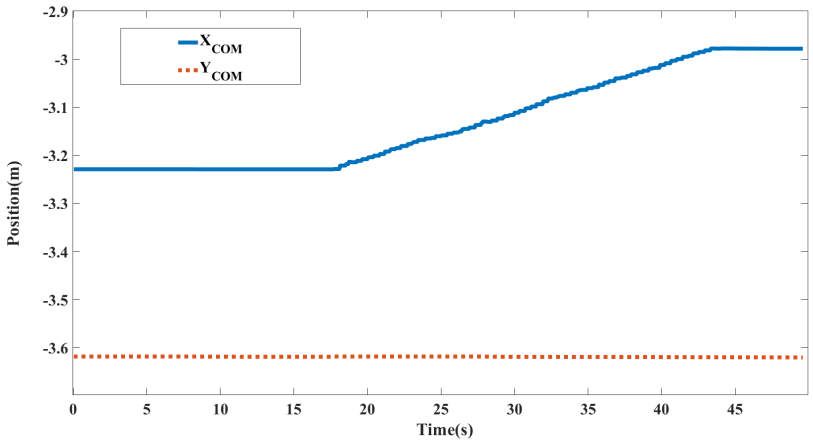

Fig. 6. Position of the floating base. Solid line represents X position of the floating base and dashed line represents Y position of floating base.

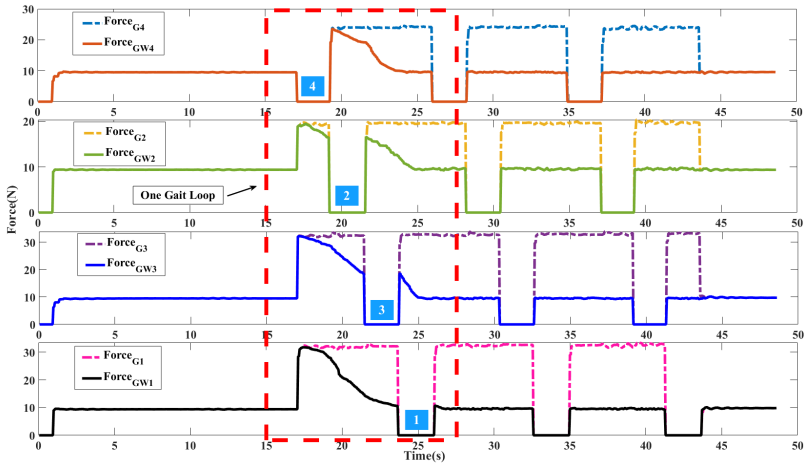

Fig. 7. Force feedback of the four effectors of the robot.The force changes of the four effectors during one gait loop {4231} are compared. The dashed line is $Force_G$, which represents the effector force change under the PD control loop, and the solid line is $Force_{GW}$, which represents the effector force change under the WBCC control loop.

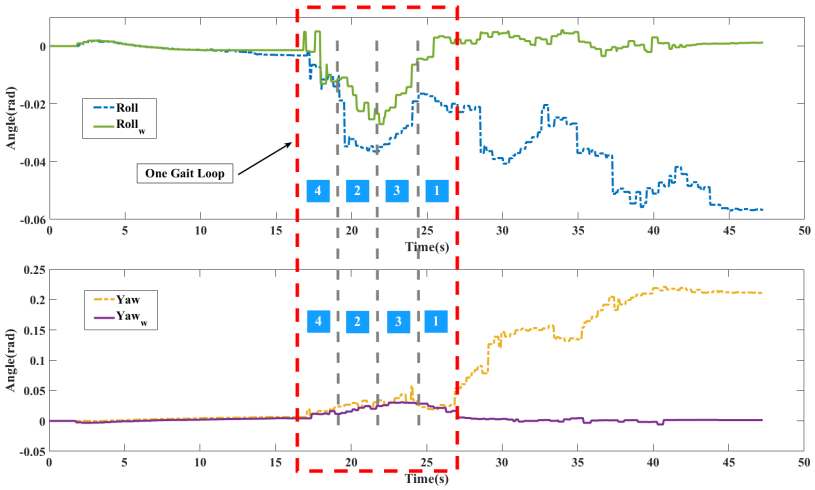

Fig. 8. Attitude of the floating base.The attitude changes of floating base during one gait loop {4231} are compared. The dashed lines represent the Roll and Yaw changes under the robot space crawling PD control loop, and the solid lines represent the attitude angle changes under the WBCC control loop.

the original 213 to 413, and according to the force diagram in Eq. (3) and Fig. 7, the rotational torque of the base surges, resulting in a large deflection of the base attitude. After using WBCC in the crawling process, combined with Fig. 7 and Fig. 8 in a gait cycle, the end effector is adjusted to stabilize the force between f_{max} and f_{climb}, and at the same time, the base deflection and pitch in the first cycle are controlled at most about 0.02 rad, and gradually converge to 0 rad with the subsequent gait adjustment. Through the above experiments, it is proved that WBCC is effective in adjusting the deflection of the base during the crawling in space.

4 Conclusions

This paper presents a WBCC strategy for multi-arm robots to achieve compliant crawling on space trusses. The strategy decomposes the compliant interaction problem during the space crawling process into an end-effector Cartesian compliance model and a floating base compliance model. By analyzing the force mapping relationship between them, a unified whole-body compliance model is established. The desired end-effector motion commands derived from this model are then optimized using MPC method to compute the optimal control torques necessary for maintaining stable contact. Simulation results demonstrate that this algorithm enhances the compliant performance of multi-arm robots, making it suitable for space truss crawling scenarios. Future work will involve validating this algorithm on a ground-based experimental setup for multi-arm space robots.

References

1. Flores-Abad, A., Ma, O., Pham, K., Ulrich, S.: A review of space robotics technologies for on-orbit servicing. J. Progress in Aerospace Sciences. 68, 1-26 (2014). doi:10.1016/j.paerosci.2014.03.002
2. Rodríguez, I., Quintero, S., Lutze, J. P., Lehner, P., Roa, M. A.: Hybrid Motion Planner for a Multi-Armed Robot Performing On-orbit Loco-manipulation Tasks. In: 2024 IEEE Aerospace Conference, pp. 1-9 (2024). doi:10.1109/AERO58975.2024.10521183
3. Huang, P., Xu, Y., Liang, B.: Dynamic balance control of multi-arm free-floating space robots. J. International Journal of Advanced Robotic Systems. 2(2), 13 (2005). doi:10.5772/5797
4. Park, J., Park, J. H.: Impedance control of quadruped robot and its impedance characteristic modulation for trotting on irregular terrain. In: 2012 IEEE/RSJ International Conference on Intelligent Robots and Systems, pp. 175-180 (2012). doi:10.1109/IROS.2012.6385710
5. Ugurlu, B., Havoutis, I., Semini, C., Caldwell, D. G.: Dynamic trot-walking with the hydraulic quadruped robot—HyQ: Analytical trajectory generation and active compliance control. In: 2013 IEEE/RSJ International Conference on Intelligent Robots and Systems, pp. 6044-6051 (2013). doi:10.1109/IROS.2013.6697234
6. Lee, J., Hyun, D. J., Ahn, J., Kim, S., Hogan, N.: On the dynamics of a quadruped robot model with impedance control: Self-stabilizing high speed trot-running and period-doubling bifurcations. In: 2014 IEEE/RSJ International Conference on Intelligent Robots and Systems, pp. 4907-4913 (2014). doi:10.1109/IROS.2014.6943260
7. Grimminger, F., Meduri, A., Khadiv, M., et al.: An open torque-controlled modular robot architecture for legged locomotion research. J. IEEE Robotics and Automation Letters. 5(2), 3650-3657 (2020). doi:10.1109/LRA.2020.2976639
8. Pratt, J., Dilworth, P., Pratt, G.: Virtual model control of a bipedal walking robot. In: Proceedings of international conference on robotics and automation, vol. 1, pp. 193-198 (1997). doi:10.1109/ROBOT.1997.620037
9. Pratt, J., Chew, C. M., Torres, A., Dilworth, P., Pratt, G.: Virtual model control: An intuitive approach for bipedal locomotion. J. The International Journal of Robotics Research. 20(2), 129-143 (2001). doi:10.1177/02783640122067309
10. Chen, G., Guo, S., Hou, B., Wang, J.: Virtual model control for quadruped robots. J. IEEE Access. 8, 140736-140751 (2020). doi:10.1109/ACCESS.2020.3013434
11. Xie, A., Chen, T., Rong, X., Zhang, G., Li, Y., Fan, Y.: A robust and compliant framework for legged mobile manipulators using virtual model control and whole-body control. J. Robotics and Autonomous Systems. 164, 104411 (2023). doi:10.1016/j.robot.2023.104411
12. Kajita, S., Nagasaki, T., Kaneko, K., Hirukawa, H.: ZMP-based biped running control. J. IEEE robotics & automation magazine. 14(2), 63-72 (2007). doi:10.1109/MRA.2007.380655
13. Tang, T., Hou, X., Xiao, Y., Su, Y., Shi, Y., Rao, X.: Research on motion characteristics of space truss-crawling robot. J. International Journal of Advanced Robotic Systems. 16(1), 1729881418821578 (2019). doi:10.1177/1729881418821578
14. Yang, S., Wen, H., Hu, Y., Jin, D.: Coordinated motion control of a dual-arm space robot for assembling modular parts. J. Acta Astronautica. 177, 627-638 (2020). doi:10.1016/j.actaastro.2020.08.006